Scholar Publishing Group
International Journal of World Medicine
https://doi.org/10.38007/IJWM.2023.040208
ISSN 2789-7133 Vol. 4, Issue 2: 63-72

Medical AGV Path Planning Based on Improved D_star Algorithm

Huiheng Suo[1,3,a], Qiang Hu[1,b], Jian Wu[1,c*], Xie Ma[2,d], Xiushui Ma[3,e*], Junhui Zhang[3,f], Jingwen Zhang[3,g], Youxuan Cai[2,h]

[1]*Nanchang Hangkong University, Nanchang, China*

[2]*Ningbo University of Finance & Economics, Ningbo, China*

[3]*NingboTech University, Ningbo, China*

[a]*suohuiheng@163.com,* [b]*1289762339@qq.com,* [c]*flywujian@qq.com,* [d]*maxie@163.com,* [e]*mxsh63@aliyun.com,* [f]*2246177205@qq.com,* [g]*1729629241@qq.com,* [h]*1337367538@qq.com*

[*]*corresponding author*

Keywords: Path Planning, D* Algorithm, Medical Robots, Cubic Spline Interpolation, Modeling and Simulation

Abstract: This paper proposes an AGV path planning algorithm for transporting medical test tubes in medical institutions. This algorithm is based on the D* algorithm and is improved with respect to cost estimation function, node selection method, and path smoothing. The feasibility of the algorithm is verified through algorithm simulation and practical application simulation.

1. Introduction

In medical institutions, test tubes are commonly used to collect and store patients' biological samples, including high-risk fluids such as blood, urine, and saliva. The AGV for transporting test tubes could replace manual labor, improve work efficiency, and reduce the risk of medical infections. In order to prevent the risk of tube leakage, the AGV for transporting test tubes needs to plan a smooth path from the starting point to the end point, while avoiding static obstacles and random dynamic obstacles as much as possible, and minimizing the vibration of the vehicle body. Therefore, path planning plays a crucial role in the completion of the test tube transport task.

Currently, The AGV path planning algorithms are mainly based on heuristic search, with A* algorithm being the most typical, and D* algorithm being developed on this basis. However, these

algorithms only consider distance cost and rarely take into account turning cost and obstacle threat cost. In addition, frequent turning of AGVs can also increase distance cost. Considering the busy working environment of test tube transport AGVs, which involves many doctors, patients, and other pedestrians, modeling pedestrian disturbance is very difficult, so this paper uses a conservative model. In order to solve the problem of path planning for test tube transport AGVs, this paper improves the traditional D* algorithm's cost estimation function, node selection method, and smooths the path using cubic spline interpolation, ensuring that the AGV completes the test tube transport task with as little vibration as possible.

2. Obstacle Threat Modeling

In this paper, obstacles that pose a threat to the trial tube transport AGV are simplified as circles, with the radius of the circle being the radius of the minimum circumscribed circle of the obstacle. Considering the lack of accurate threat parameters, some margin is left for all threats.

$$J(X)=\begin{cases}0 & D>R+2\\ 2^{(R-D)^2} & R\le D\le R+2\\ +\infty & D<R\end{cases} \tag{1}$$

Where, $J(X)$ is the obstacle threat cost of AGV established through static map, R is the threat radius of obstacles, D is the distance from the current position of AGV to the center of the obstacle.

3. Improved D* Algorithm

3.1. Improvement of Cost Estimation Function

The improved cost estimation function of the D* algorithm is given by equation (2).

$$\mathrm{f}(X,R)=ah(X)+bg(X,R) \tag{2}$$

Where, $h(X)$ represents the cost from the target point to point X, while $\mathrm{g}(X,R)$ represents the cost from point X to the current position of AGV [1][3].

Considering the actual usage of the AGV, frequent turning not only easily deviates the AGV from the planned path and elongates its travel trajectory but also increases the risk of medical liquid leakage. Moreover, in the case of multiple AGVs handling, frequent changes in direction may result in collisions. Therefore, the cost estimation should take into account the turning angle during the AGV's travel process [2]. The modified cost estimation function is shown in equation (3).

$$\mathrm{f}(X,R)=ah(X)+bg(X,R)+cthr(X) \tag{3}$$

Where, $thr(X)$ refers to the heading deviation angle at point x, which can be calculated using the quaternion $\mathrm{q}=(x,y,z,w)$, as shown in the following formula.

$$\mathrm{thr}\ (\mathrm{X})=\left|\arctan\left(\frac{\mathrm{goal}Y}{\mathrm{goal}X}\right)-\arctan\left(\frac{2(\mathrm{wz}+\mathrm{xy})}{1-2(\mathrm{y}^2+\mathrm{z}^2)}\right)\right| \tag{4}$$

Where, $goalY$ represents the y-coordinate of the target point in the absolute coordinate system, while $goalX$ represents the x-coordinate of the target point in the absolute coordinate system.

Considering the threat cost of obstacles, the heuristic function of the improved D* algorithm should be modified to:

$$\mathrm{f}(X,R)=a\mathrm{h}(X)+bg(X,R)+cthr(X)+dJ(X) \tag{5}$$

The traditional D* algorithm commonly uses Euclidean distance as the cost value. In a two-dimensional space, the expression for the Euclidean distance between points (x_1,y_1) and (x_2,y_2) is as follows:

$$l_{Euclidean}=\sqrt{(x_1-x_2)^2+(y_1-y_2)^2} \tag{6}$$

Observing formula (6), it can be seen that calculating the Euclidean distance requires a square root operation, which increases the computation time of the program. Furthermore, the Euclidean distance is essentially the straight-line distance between two points in two-dimensional space [4], without taking into account the heading angle information of the medical transport AGV during operation, which results in a path with multiple turns being planned. Therefore, this paper optimizes the cost estimation function by using the Chebyshev distance instead of the Euclidean distance. In two-dimensional space, the Chebyshev distance between points (x_1,y_1) and (x_2,y_2) is expressed as follows [5]:

$$l_{Chebyshev}=\max\left\|x_2-x_1\right|,\left|y_2-y_1\right\| \tag{7}$$

The optimized cost estimation function can be obtained as follows, where the vertical and horizontal cost values are set as 1, and the diagonal cost value is set as 1.41 to avoid square root operation and improve algorithm efficiency.

$$h(X)=1.41\min(\left|x_2-x_1\right|,\left|y_2-y_1\right|)+\left\|x_2-x_1\right|-\left|y_2-y_1\right\| \tag{8}$$

Based on the considerations mentioned above, we can obtain the final improved cost estimation function as follows:

$$\begin{aligned}&\mathrm{f}(X,R)=a(1.41\min(\left|x_2-x_1\right|,\left|y_2-y_1\right|)+\left\|x_2-x_1\right|-\left|y_2-y_1\right\|)\\&+bg(X,R)\\&+c\left|\arctan\left(\frac{\mathrm{goal}Y}{\mathrm{goal}X}\right)-\arctan\left(\frac{2(\mathrm{wz}+\mathrm{xy})}{1-2(\mathrm{y}^2+\mathrm{z}^2)}\right)\right|\\&+dJ(X)\end{aligned} \tag{9}$$

3.2. Improvement of the Node Selection Method

In traditional D* algorithm, the current node is taken as the parent node, and the 8 neighboring child nodes of the parent node are selected for expansion operation, and all 8 child nodes have the same priority as expansion options. However, since the cost of expansion in the diagonal direction is lower, it indirectly leads to the path passing between two obstacles. Considering the practical application scenario, passing between obstacles can easily lead to collisions of AGVs and increase the risk of medical liquid leakage. Therefore, this paper proposes an improvement by dividing the selection of child nodes into two levels: preferred child nodes and alternative child nodes.

Choosing $Node2$, $Node4$, $Node5$, $Node7$ as the preferred child nodes, as shown in Figure 1:

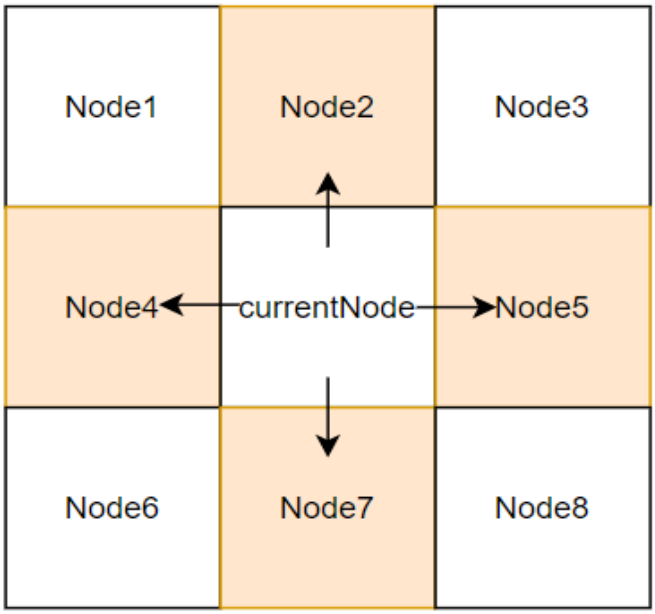

Figure 1. Node expansion diagram

*N*ode1 *N*ode3 *N*ode6 *N*ode8 are selected as alternative child nodes. The preferred child node is the node that is prioritized for expansion, and an alternative child node follows the following requirements:

(1) If *N*ode2 is an obstacle, *N*ode1 and *N*ode3 are prohibited.
(2) If *N*ode4 is an obstacle, *N*ode1 and *N*ode6 are prohibited.
(3) If *N*ode5 is an obstacle, *N*ode3 and *N*ode8 are prohibited.
(4) If *N*ode7 is an obstacle, *N*ode6 and *N*ode8 are prohibited.

3.3. Path Smoothing

Considering that path planners usually just connect the planned path points with straight lines and ignore the requirement of producing as little vibration as possible during the AGV's motion, this paper uses a cubic spline interpolation method to smooth the path and make the AGV travel as smoothly as possible. Although the condition of cubic spline interpolation is that the abscissas of each interpolated point should be different, the sequence of planned path points obtained by the path planning algorithm is not necessarily subject to this restriction. In order to achieve a smooth path, this paper adopts a method of segmenting the planned path point sequence and performing cubic spline interpolation on each segment. The specific steps are shown in Figure 2.

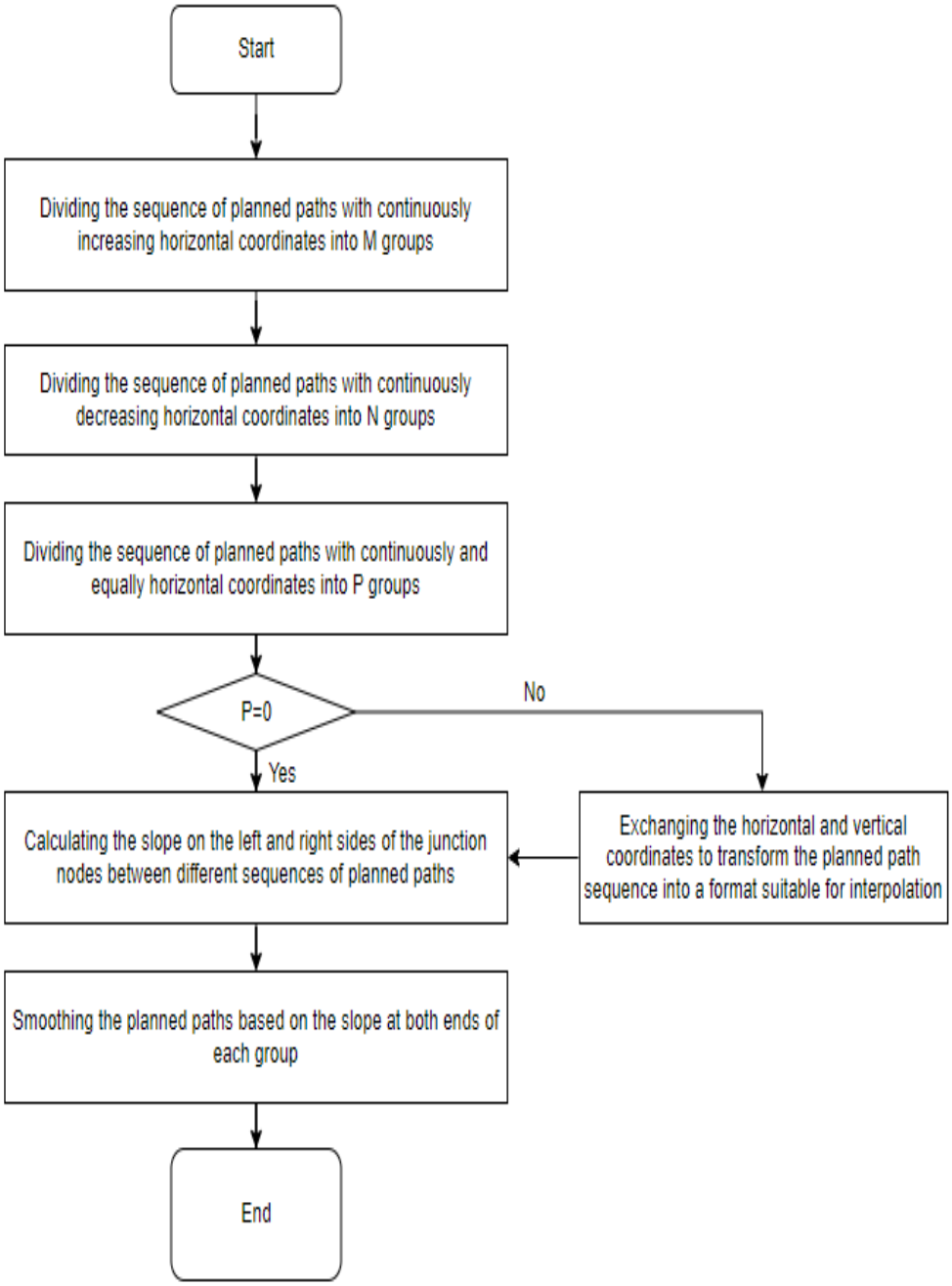

Figure 2. Path smoothing process flowchart

3.4. Improvement Summary of D* Algorithm

Taking into account the improvements discussed earlier, the flowchart for the improved D* algorithm is shown in Figure 3.

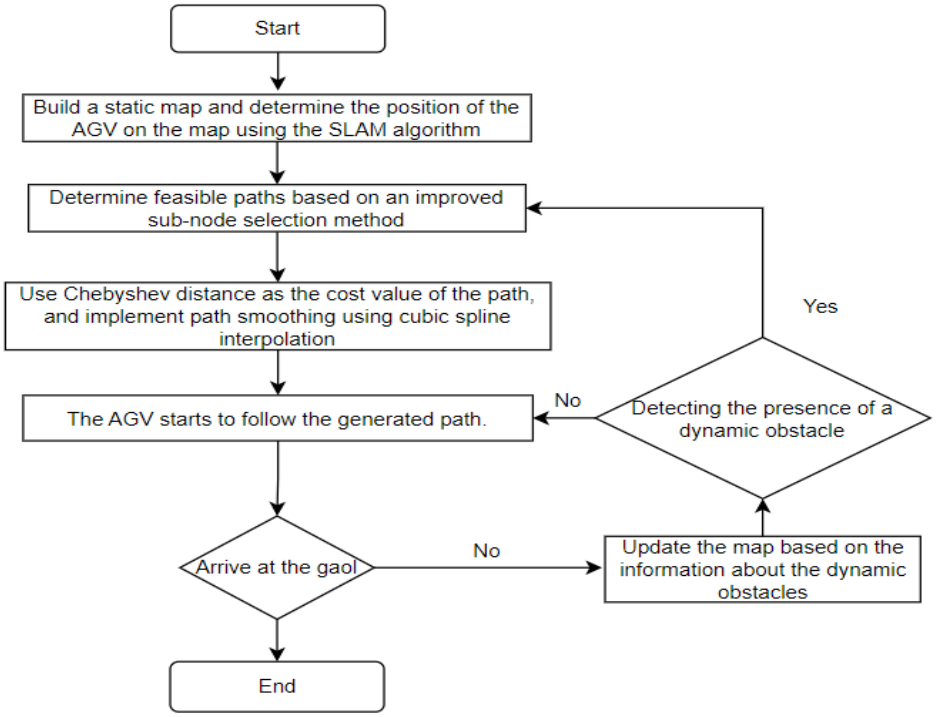

Figure 3. Improved D Algorithm Flowchart*

4. Simulation Results and Analysis

4.1. Algorithm Simulation Environment

To validate the feasibility of the proposed algorithm in this paper, a simulated medical environment for the operation of medical AGVs was established, and the static map is shown in Figure 3. The purple circles represent static obstacles, while the black circles represent dynamic obstacles. In this paper, the AGV is idealized as a point without size, and the obstacles are inflated with a circle of shadows around them to represent the collision radius of the AGV, which is equal to the minimum circumscribed circle radius of the AGV, in order to ensure the correctness of the simulation. The starting point of the AGV is $(9,9)$, and the endpoint is $(90,90)$.

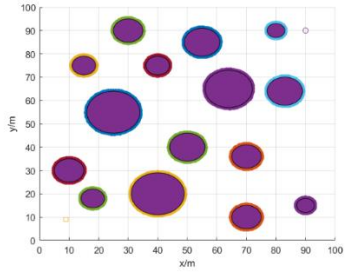

Figure 4. AGV driving environment

4.2. Algorithm Simulation Results Analysis

If there are no dynamic obstacles in the AGV's operating environment, that is, the static map is exactly the same as the actual environment, then the algorithm degenerates into the A* algorithm, and the planned path is shown in Figure 5. From the figure, it can be seen that the AGV avoids

obstacles while minimizing turns, allowing for smooth arrival at the destination.

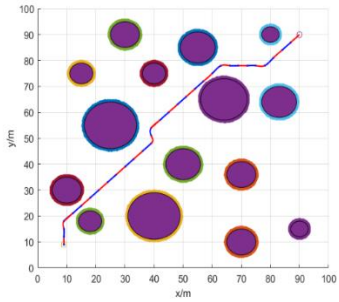

Figure 5. The planned path generated under the condition of no dynamic obstacles

When there are different numbers of dynamic obstacles present, the simulation results of the algorithm are shown in Figures 6-9:

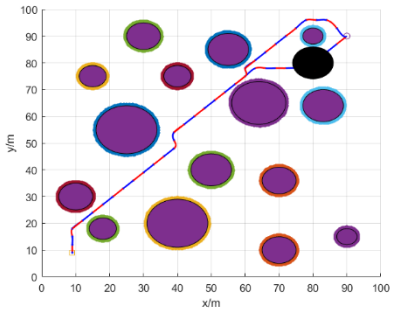

Figure 6. Path planned with 1 dynamic obstacle present

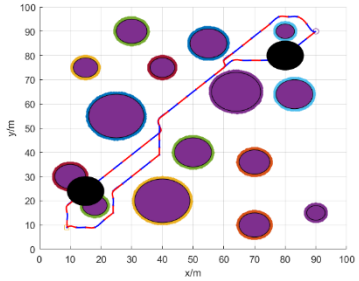

Figure 7. Path planned with 2 dynamic obstacles present

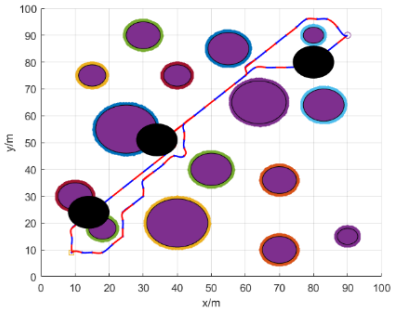

Figure 8. Path planned with 3 dynamic obstacles present

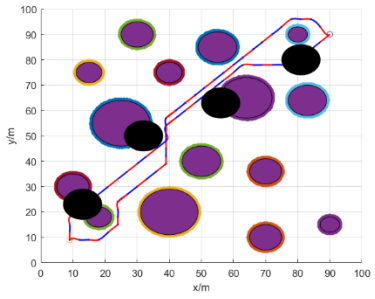

Figure 9. Path planned with 4 dynamic obstacles present

4.3. Simulation of Medical Application Scenarios

Now consider the following usage scenario for the medical AGV: Firstly, the AGV needs to retrieve a test tube containing patient saliva from the conveyor belt. However, due to emergency construction, there are obstacles on the way from the AGV's starting point to the conveyor belt that were not known beforehand. After loading the test tube, the AGV needs to pass through a crowded corridor and deliver the test tube to the laboratory. Here, it is assumed that pedestrians will not actively avoid the AGV, so the AGV must achieve autonomous obstacle avoidance. The simulation

scenario is shown in Figure 10.

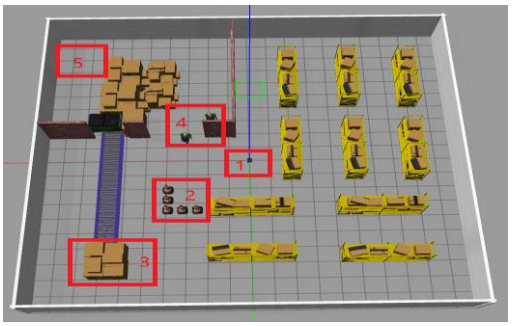

Figure 10. AGV medical application environment

In Figure 10, box 1 represents the starting position of the AGV, box 2 is an unknown obstacle added due to emergency construction, box 3 is the location where the AGV loads the patient's saliva, box 4 is where moving medical staff and patients need to be dynamically avoided, and box 5 is the laboratory, which is the endpoint of the AGV.

According to the simulation of this usage scenario, as shown in Figures 11- 17:

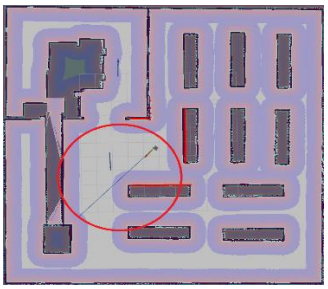

Figure 11. Planned path of AGV to the conveyor belt

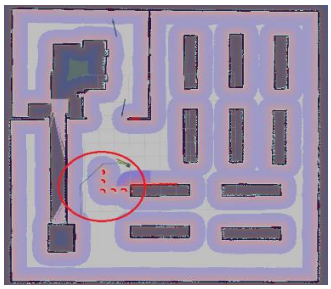

Figure 12. Planned path of AGV after discovering an unknown obstacle

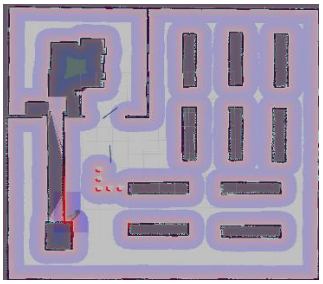

Figure 13. AGV has obtained the test tubes

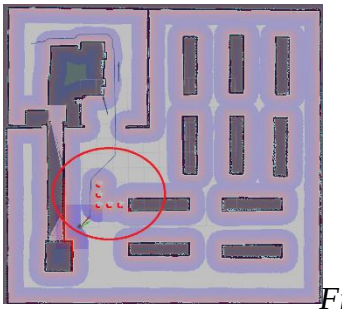

Figure 14. AGV's plan to laboratory

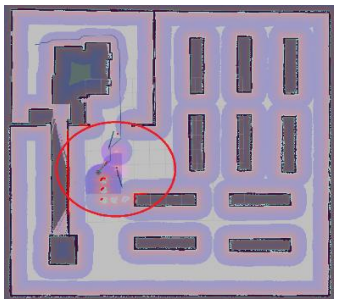

Figure 15. Path diagram of the first route planned by AGV to avoid pedestrians

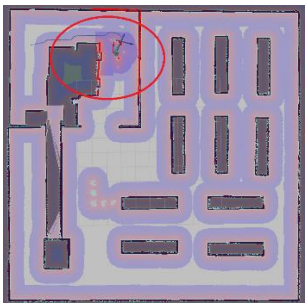

Figure 16. Path diagram of the route planned by AGV to avoid pedestrians

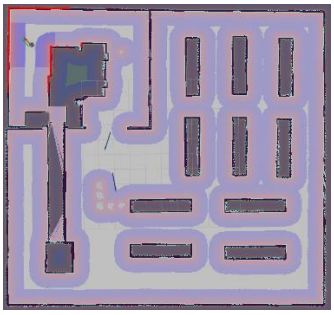

Figure 17. AGV successfully arrived at the laboratory

In Figure 11, since there were no construction obstacles in the static map, the path planned by the AGV to the conveyor belt was almost a straight line. In Figure 12, the AGV discovered an obstacle and started a second planning of the route, avoiding the obstacle. In Figure 13, the AGV successfully picked up the obstacle and waited for commands from the upper computer. In Figure 14, the AGV started planning the path to the laboratory. As shown in Figure 3, the static map was updated with the construction obstacle information, but there was no information about pedestrian obstacles. Therefore, the path planned in this case only avoided the construction obstacles without considering pedestrian obstacles. In Figures 15 and 16, the AGV noticed pedestrians nearby and modified its path for obstacle avoidance. In Figure 17, the AGV successfully reached the laboratory and completed the transportation task.

5. Conclusions

In order to reduce the risks of increased distance, collisions, and medical liquid leaks caused by frequent turning in medical AGV transportation tasks, this paper adds a turning cost to the cost estimate function of the D* algorithm and improves the selection of sub-nodes. At the same time, to make the AGV stay as far away as possible from threatening obstacles, an obstacle threat cost is introduced into the cost function of the algorithm. Simulation results show that the improved algorithm reduces the total heading angle and threat cost. Considering that AGV needs to generate as little vibration as possible, in order to obtain a smooth path, this paper uses the cubic spline interpolation algorithm to smooth the route. Through algorithm simulation and actual application simulation verification, this algorithm achieves the expected effect.

Funding

This paper is supported by Projects of major scientific and technological research of Ningbo City(2020Z065, 2021Z059,2022Z056,2023Z050(the second batch)), Major instrument special projects of the ministry of science and technology of China(2018YFF01013200), Projects of major scientific and technological research of Beilun District, Ningbo City(2021BLG002, 2022G009), Projects of engineering research center of Ningbo City (Yinzhou District Development and Reform Bureau [2022] 23), Projects of scientific and technological research of colleges student's of China(202213001008).

Data Availability

Data sharing is not applicable to this article as no new data were created or analysed in this study.

Conflict of Interest

The author states that this article has no conflict of interest.

References

[1] *Wu Jian, Zhang Donghao. UAV Route Planning and Smoothing Based on Improved D * Algorithm. Aerospace Science and Technology, 2013 (6): 69-71.*

[2] *Zhang Donghao. Research on Route Planning Technology for Unmanned Aerial Vehicles in Complex Situations .Nanchang: Nanchang Hangkong University, 2014.*

[3] *Cao Y, Long T, Wang Z, et al. Aircraft route planning for stealth penetration based on sparse A search//2017 29th Chinese Control and Decision Conference (CCDC). IEEE, 2017: 5380-5385.*

[4] *Farrand W H, Bell III J F, Johnson J R, et al. VNIR multispectral observations of rocks at Cape York, Endeavour crater, Mars by the Opportunity rover's Pancam. Icarus, 2013, 225(1): 709-725.*

[5] *Dai Nianhui, Zhao Jiangming, Wangaojie. An Improved Method for Path Planning Based on D * Lite Algorithm. Machine Tool and Hydraulic, 2022, 50(2): 167-171.*